LETTER

Synthesis, Crystal Structure and Antifungal Activity of New Furan-1,3,4-oxadiazole Carboxamide Derivatives①

SUN Yue YANG Zi-Hui GU Wen②

(*Jiangsu Provincial Key Lab for the Chemistry and Utilization of Agro-forest Biomass, Jiangsu Key Lab of Biomass-based Green Fuels and Chemicals, Co-inovation Center for Efficient Processing and Utilization of Forest Products, College of Chemical Engineering, Nanjing Forestry University, Nanjing* 210037, *China*)

ABSTRACT A series of novel furan-1,3,4-oxadiazole carboxamide derivatives (**5a**～**5e**) were designed, synthesized and characterized by spectroscopic methods including HR-MS, ^{1}H- and ^{13}C-NMR. The crystal structure of compound **5a** was determined by single-crystal X-ray diffraction. The compound crystallizes in the triclinic system, space group $P\bar{1}$ with a = 4.7261(5), b = 10.4672(11), c = 14.5886(13) Å, α = 106.081(4)°, β = 91.043(3)°, γ = 99.456(4)°, Z = 2, V = 682.48(12) Å^3, M_r = 348.16, D_c = 1.694 Mg/m^3, S = 1.008, m= 3.025 mm^{-1}, F(000) = 348, the final R = 0.0775 and wR = 0.2080 for 2774 observed reflections ($I > 2\sigma(I)$). There are two kinds of hydrogen bonds (N(3)–H(3A)⋯N(2) and C(8)–H(8A)⋯O(3)) present in its crystal structure. The preliminary antifungal assay showed that compounds **5b** and **5c** exhibited significant antifungal activities against several plant pathogenic fungi.

Keywords: furan-1,3,4-oxadiazole carboxamide, synthesis, crystal structure, antifungal activity;

DOI: 10.14102/j.cnki.0254-5861.2011-3232

1 INTRODUCTION

Antifungal agrochemicals have been playing an important role in reducing the huge losses in agricultural production caused by plant diseases. Nowadays, the application of antifungal agrochemicals meets the progressive reduction of efficiency due to the increasing resistance by pathogenic fungi[1, 2]. Therefore, there is still an urgent need to develop new antifungal agents with better efficacy against plant pathogens.

Heterocyclic compounds have drawn extensive interests in the development of medicines and pesticides because of their prominent physiochemical and pharmaceutical properties[3-5]. Oxadiazole derivatives received increasing attention due to their various biological activities, such as antitumor[6], antibacterial[7], antifungal[8], insecticidal[9] and herbicidal activities[10]. Furan moiety is also a key building block in many drugs or pesticides due to its biological activities including antimicrobial[11], antitumor[12, 13], antioxidant[14], antimalarial[15], fungicidal[16-18] and herbicidal properties[19, 20]. Lots of furan compounds were developed as commercial medicines or pesticides such as fenfuram and furalaxyl. In addition, carboxamide is also a key building block in many drugs or pesticides, for example, fluopyram, penflufen, bixafen and fluxapyroxad. Especially, aromatic carboxamide derivatives have attracted great attention since a number of carboxamide derivatives, such as thifluzamide, isopyrazam and benodanil, were commercialized as fungicides for crop protection. Recently, Zhu et al designed and synthesized the novel compound containing the carboxamide group that exhibited impressive spore germination inhibitory properties[21]. Yu et al. also synthesized a series of pyrazole-thiazole carboxamides which showed promising *in vivo* antifungal activity against *Rhizoctonia solani*[22].

Based on these findings, a series of novel furan-1,3,4-oxadiazole carboxamide derivatives were synthesized as potential antifungal agents. Their structures were characterized by ^{1}H-NMR, ^{13}C-NMR and HR-MS spectra, and the crystal structure of one title compound was determined by single-crystal X-ray diffraction analysis. The *in vitro* anti-

Received 23 April 2021; accepted 29 June 2021 (**CCDC 2076125**)

① This work was supported by the National Natural Science Foundation of China (31770616) and the Natural Science Foundation for Colleges and Universities in Jiangsu Province (17KJA220002). The authors would thank the Modern Analysis and Testing Center, Nanjing Forestry University for NMR test

② Corresponding author. Gu Wen, born in 1979, Ph. D., professor, majoring in synthetic medicinal chemistry. E-mail: njguwen@163.com

fungal activities of the title compounds against several crop pathogenic fungi were also preliminarily evaluated.

2 EXPERIMENTAL

2. 1 Reagents and measurements

The melting points were determined by an XT-4 melting point apparatus (Taike Corp., Beijing, China) and were uncorrected. ^{1}H-NMR and ^{13}C-NMR spectra were obtained by using a Bruker AV-600 spectrometer (Bruker Co. ltd, Switzerland) with TMS as the internal standard. The crystal structure was recorded on a Bruker APEXII CCD diffractometer. High-resolution mass spectrometry (HRMS) data were obtained on a Waters G2-xs (LC/ESI) instrument (Waters, United States). SP-300B Biochemistry incubator (Nanjing Hengyu Co., Ltd., China) was used for *in vitro* antifungal assay. Reactions were monitored by TLC which was carried out on silica gel IB-F flexible sheets (Mallinckrodt Baker Inc., Germany) and visualized in UV light (254 and 365 nm). Silica gel (300～400 mesh) for column chromatography was purchased from Qingdao Marine Chemical Factory, China. The reagents and chemicals of AR grade were purchased from commercial suppliers and used without further purification.

2. 2 Synthesis of the title compounds 5a～5e

The synthetic route for compounds **5a**～**5e** was outlined in Scheme 1. The intermediate **2** was synthesized according to the method in the previous report[23]. To a solution of compound **2** (7.0 mmol) and Et_3N (14.0 mmol) in 10 mL of anhydrous CH_2Cl_2 was added methyl oxalyl chloride (7.7 mmol) dropwise in an ice bath. The mixture was stirred at 0 ℃ for 30 min and then stirred at room temperature for 14 h. At the end of reaction, the solvent was evaporated to give a crude product of compound **3** which could be used directly for the next step. The intermediate **3** was re-dissolved with 15 mL of $POCl_3$, and the reaction mixture was refluxed for 15 h. Then the mixture was cooled to room temperature and poured slowly into ice water (50 mL). The mixture was stirred for 15 minutes and then the precipitate formed was filtered and dried to afford compound **4**. Subsequently, to a solution of compound **4** (1.0 mmol) in DMF (10 mL) was added different substituted benzylamine (1.2 mmol). The mixture was stirred at 80 ℃ for 2～5 h. At the completion of reaction, the mixture was cooled to room temperature and poured into ice water (50 mL), and the solid was filtered and dried. Finally, the crude product was recrystallized from petroleum ether and ethanol to give the title compounds **5a**～**5e**.

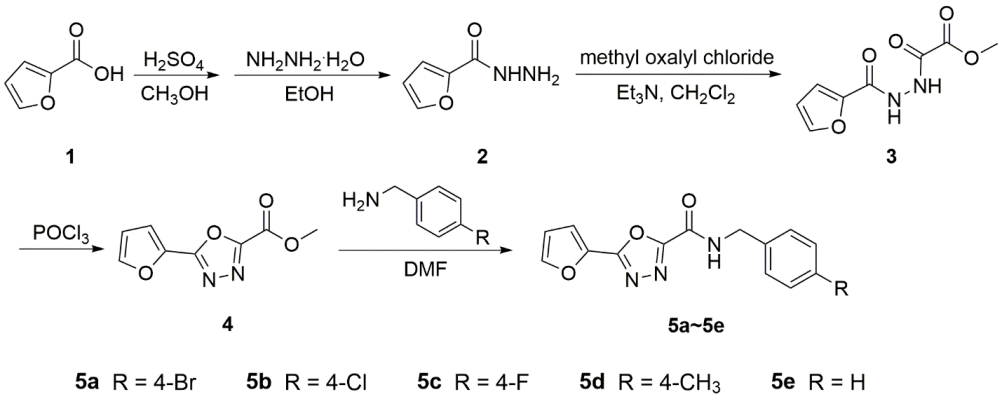

Scheme 1. Synthetic route of compounds 5a～5e

Compound **5a**: Yellow solid; yield, 66%, m.p. 165～166 ℃; ^{1}H-NMR (600 MHz, DMSO-d_6) δ 4.45 (d, J = 6.2 Hz, 2H), 6.84 (dd, J = 3.6, 1.7 Hz, 1H), 7.32 (d, J = 8.4 Hz, 2H), 7.48 (d, J = 3.5 Hz, 1H), 7.54 (d, J = 8.4 Hz, 2H), 8.12 (d, J = 1.1 Hz, 1H), 9.91 (t, J = 6.1 Hz, 1H); ^{13}C-NMR (150 MHz, DMSO-d_6) δ 42.0, 112.9, 115.9, 120.1, 129.7, 131.2, 137.8, 138.1, 147.7, 153.0, 157.5, 157.8; ESI-HRMS: *m*/*z* calcd. for $C_{14}H_{11}BrN_3O_3$ $[M+H]^+$: 347.9984; found: 347.9981.

Compound **5b**: Yellow solid; yield, 85%, m.p. 136.5～138.5 ℃; ^{1}H-NMR (600 MHz, DMSO-d_6) δ 4.47 (d, J = 6.2 Hz, 2H), 6.84 (dd, J = 3.5, 1.7 Hz, 1H), 7.37 (d, J = 8.5 Hz, 2H), 7.41 (d, J = 8.5 Hz, 2H), 7.48 (d, J = 3.5 Hz, 1H), 8.12 (s, 1H), 9.91 (t, J = 6.1 Hz, 1H); ^{13}C-NMR (150 MHz, DMSO-d_6) δ 41.9, 112.9, 115.9, 128.3, 129.3, 131.6, 137.4, 138.1, 147.7, 153.0, 157.6, 157.8; ESI-HRMS: *m*/*z* calcd. for $C_{14}H_{11}ClN_3O_3$: 304.0489 $[M + H]^+$; found 304.0493.

Compound **5c**: White solid; yield, 84%, m.p. 137.1～

139.5 ℃; ^{1}H-NMR (600 MHz, DMSO-d_6) δ 4.46 (d, J = 6.2 Hz, 2H), 6.84 (t, J = 3.8, 1.7 Hz, 1H), 7.17 (t, J = 8.9 Hz, 2H), 7.39 (dd, J = 8.4, 5.7 Hz, 2H), 7.48 (d, J = 3.5 Hz, 1H), 8.12 (s, 1H), 9.90 (t, J = 6.0 Hz, 1H); ^{13}C-NMR (150 MHz, DMSO) δ 42.4, 113.4, 115.5 (d, J = 21.1 Hz), 116.4, 130.0 (d, J = 8.1 Hz), 135.0 (d, J = 2.9 Hz), 138.6, 148.2, 153.4, 158.1, 158.3, 161.8 (d, J = 241.0 Hz); ESI-HRMS: *m*/*z* calcd. for $C_{14}H_{11}FN_3O_3$: 288.0784 $[M + H]^+$; found 288.0781.

Compound **5d**: White solid; yield, 86%, m.p. 149.5～151.2 ℃; ^{1}H-NMR (600 MHz, DMSO-d6) δ 2.28 (s, 3H), 4.43 (d, J = 6.2 Hz, 2H), 6.84 (dd, J = 3.0, 1.2 Hz, 1H), 7.14 (d, J = 7.8 Hz, 2H), 7.23 (d, J = 7.8 Hz, 2H), 7.47 (d, J = 3.5 Hz, 1H), 8.12 (s, 1H), 9.85 (t, J = 6.1 Hz, 1H); ^{13}C-NMR (150 MHz, DMSO-d6) δ 20.6, 42.3, 112.9, 115.9, 127.4, 128.8, 135.3, 136.1, 138.1, 147.6, 152.8, 157.6, 157.8; ESI-HRMS: *m*/*z* calcd. for $C_{15}H_{14}N_3O_3$ $[M + H]^+$: 284.1035; found 284.1039.

Compound **5e**: White solid; yield, 43%, m.p. 148～149.5 ℃; ^{1}H-NMR (600 MHz, DMSO-d_6) δ 4.48 (d, J = 6.2 Hz, 2H), 6.84 (dd, J = 3.4, 1.6 Hz, 1H), 7.26 (m, 1H), 7.33～7.35 (m, 4H), 7.48 (d, J = 3.5 Hz, 1H), 8.12 (s, 1H), 9.89 (t, J = 6.1 Hz, 1H); ^{13}C-NMR (150 MHz, DMSO-d_6) δ 42.5, 112.9, 115.9, 127.0, 127.4, 128.3, 138.1, 138.3, 147.7, 152.9, 157.6, 157.8; ESI-HRMS: *m*/*z* calcd. for $C_{14}H_{12}N_3O_3$ $[M+H]^+$: 270.0879; found 270.0880.

2. 3 X-ray structure determination

The crystals suitable for X-ray diffraction were obtained by slow evaporation of the solutions of the title compound **5a** in petroleum ether/ethanol at room temperature. X-ray diffraction data were collected on a Bruker APEXII CCD diffractometer equipped with graphite-monochromated Mo$K\alpha$ radiation (λ = 0.71073 Å) by using φ and ω scan modes in the range of $2.06 \leqslant \theta \leqslant 28.24°$ ($-6 \leqslant h \leqslant 6$, $-13 \leqslant k \leqslant 13$, $-19 \leqslant l \leqslant 19$) at 296(2) K. A total of 6166 reflections were collected, of which 3302 were independent (R_{int} = 0.0579) and 2774 were observed with $I > 2\sigma(I)$. The structure was solved by direct methods using SHELXS-2014/7 and refined by full-matrix least-squares procedure on F^2 with SHELXL-2014/7. All non-hydrogen atoms were refined anisotropically using all reflections with $I > 2\sigma(I)$. All H atoms were generated geometrically and refined in terms of the riding model. The final refinement gave R = 0.0775, wR = 0.2080 ($w = 1/[\sigma^2(F_o^2) + (0.0580P)^2]$, where $P = (F_o^2 + 2F_c^2)/3$, S = 1.008, $(\Delta/\sigma)_{max}$ = 0.000, $(\Delta\rho)_{max}$ = 1.506 and $(\Delta\rho)_{min}$ = –1.537 e/Å^3. The selected bond distances and bond angles are listed in Table 1.

Table 1. Selected Bond Lengths (Å) and Bond Angles (°) of Compound 5a

Bond	Dist.	Bond	Dist.	Bond	Dist.
Br–C(12)	1.912(4)	N(2)–C(6)	1.281(5)	C(4)–C(5)	1.446(6)
N(1)–C(5)	1.290(6)	O(2)–C(6)	1.363(5)	C(6)–C(7)	1.498(6)
N(1)–N(2)	1.402(6)	C(2)–C(3)	1.451(10)	C(8)–C(9)	1.513(6)
O(1)–C(4)	1.352(6)	O(3)–C(7)	1.209(5)	C(9)–C(10)	1.386(6)
O(1)–C(1)	1.363(8)	N(3)–C(7)	1.346(5)	C(10)–C(11)	1.388(7)
C(1)–C(2)	1.314(12)	N(3)–C(8)	1.457(6)	C(11)–C(12)	1.381(7)
Angle	(°)	Angle	(°)	Angle	(°)
C(5)–N(1)–N(2)	105.2(4)	C(1)–C(2)–C(3)	108.7(5)	O(2)–C(6)–C(7)	117.1(3)
C(4)–O(1)–C(1)	106.4(5)	C(7)–N(3)–C(8)	121.7(3)	O(3)–C(7)–N(3)	126.8(4)
C(2)–C(1)–O(1)	109.8(6)	C(3)–C(4)–C(5)	129.0(5)	N(3)–C(8)–C(9)	113.2(3)
C(5)–O(2)–C(6)	101.9(3)	N(1)–C(5)–O(2)	113.5(4)	C(11)–C(12)–C(13)	122.0(4)
C(6)–N(2)–N(1)	106.8(4)	N(2)–C(6)–O(2)	112.6(4)	C(11)–C(12)–Br	119.3(3)
O(1)–C(1)–C(2)–C(3)	−0.5(7)	N(1)–N(2)–C(6)–O(2)	0.5(5)	C(7)–N(3)–C(8)–C(9)	92.3(5)
C(1)–C(2)–C(3)–C(4)	0.0(7)	N(2)–C(6)–C(7)–N(3)	−2.9(6)	N(3)–C(8)–C(9)–C(10)	−72.5(5)
O(1)–C(4)–C(5)–N(1)	−2.3(7)	C(8)–N(3)–C(7)–O(3)	1.9(7)	C(10)–C(11)–C(12)–Br	177.8(4)

2. 4 Antifungal activity

Antifungal activities of compounds **5a**～**5e** were tested *in vitro* against seven plant pathogenic fungi including *Rhizoctonia solani* (*R. solani*), *Botrytis cinerea* (*B. cinerea*), *Fusarium oxysporum* (*F. oxysporum*), *Sclerotinia sclerotiorum* (*S. sclerotiorum*), *Colletotrichum capsici* (C. *capsici*), *Alternaria solani* (*A. solani*) and *Gibberella zeae* (*G. zeae*), which were provided by the Agricultural Culture Collection of China (ACCC). These tests were carried out by an mycelia growth inhibition method, and the procedures are consistent with the literature[24, 25]. The stock solution was added into PDA medium, and the concentration of target compounds was 50 mg/L. Pure DMSO without the target compounds was added into PDA medium as blank control,

and boscalid was co-assayed as positive control. Fresh dishes with a diameter of 5 mm were taken from the edge of the PDA-cultured fungal colonies, and inoculated on the above three PDA media. Each treatment was processed for three replicates, and the fungicidal effect was averaged. Their relative inhibitory rate I(%) was calculated according to the following equation: $I(\%) = [(C–T)/(C–5)] \times 100$, where I is the inhibitory rate, C the colony diameter of the control (mm), and T the colony diameter of treatment (mm).

3 RESULTS AND DISCUSSION

In this work, 2-furan carboxylic acid (**1**) was used as the starting material, which was converted to the corresponding hydrazide (**2**) by successive methyl esterification and hydrazidation reactions. Compound **2** reacted with methyl oxalyl chloride to afford intermediate **3**, which was subjected to an intramolecular cyclization to give the furan-1,3,4-oxadiazole derivative **4** with the yield of 90%. Subsequently, the title compounds **5a**～**5e** were obtained by reacting compound **4** with different substituted benzylamine in 43～86% yield.

The structures of compounds **5a**～**5e** were characterized by its HR-MS, ^{1}H- and ^{13}C-NMR spectroscopic data. As for a typical example, the molecular formula of compound **5a** was determined as $C_{14}H_{10}BrN_3O_3$ through HR-MS spectrum (m/z $[M+H]^+$ calcd. for $C_{14}H_{11}BrN_3O_3$: 347.9984; found: 347.9981). In the ^{1}H-NMR data, the appearance of doublet at δ 4.45 ppm belongs to the methylene protons of benzyl moiety. Two doublets at δ 8.12 and 7.48 ppm and the double doublet at δ 6.84 ppm can be attributed to three aromatic protons of furan ring at C(1), C(3) and C(2), respectively, while two doublets each containing two protons at δ 7.32 and 7.54 ppm are due to the protons of the phenyl ring at C(10)/C(14) and C(11)/C(13), respectively. In addition, the triplet with one proton at δ 9.91 ppm can be attributed to the carboxamide proton. The ^{13}C-NMR spectrum of compound **5a** exhibits 12 well resolved resonances for 14 carbon atoms. Among them, the absorption peak at δ 42.0 ppm is corresponding to the methylene carbon (C(8)), and four peaks at δ 120.1, 129.7 (2C), 131.2 (2C) and 137.8 ppm are attributed to the six carbons at the benzene ring (C(9)～C(14)). On the other hand, four peaks at δ 112.9, 115.9, 138.1 and 147.7 ppm can be assigned to the carbons in the furan ring (C(1)～C(4)), while the three peaks at δ 153.0, 157.5 and 157.8 ppm are the signals of C(5), C(6) in the oxadiazole ring and the signal of amide carboxyl carbon (C(7)), respectively. The assignments of the signals in the ^{1}H- and ^{13}C-NMR spectra of compound **5a** are in good accordance with its structure. Moreover, the structures of compounds **5b**～**5e** can also be characterized by their spectral data in a similar manner.

The perspective view of compound **5a** with atomic numbering scheme is given in Fig. 1, and the selected bond lengths and bond angles are listed in Table 1. As shown in Table 1, the bond lengths and bond angles within the furan and oxadiazole rings agreed well with the normal values. The dihedral angle between the furan (O(1), C(1)～C(4)) and oxadiazole rings (N(1), C(5), O(2), C(6), N(2)) is 2.88(38)°, indicating that they are coplanar. In addition, the torsion angles N(2)–C(6)–C(7)–N(3) and O(2)–C(6)–C(7)–O(3) are −2.9(6)° and −4.1(6)°, respectively, which indicated that the amide moiety is also coplanar with the oxadiazole ring. The bond length of N(3)–C(7) is 1.346(5) Å, shorter than the isolated N–C single bond (1.471 Å) but longer than the double bond (1.273 Å) due to the p-π conjugation effect between the nitrogen atom and the carboxyl group. Owing to the existence of sp^3-hybrid methylene carbon (C(8)), the benzene ring (C(9)～C(14)) is not coplanar with the furan-1,3,4-oxadiazole carboxamide moiety, causing a dihedral angle of 66.99(16)° between the benzene and oxadiazole rings.

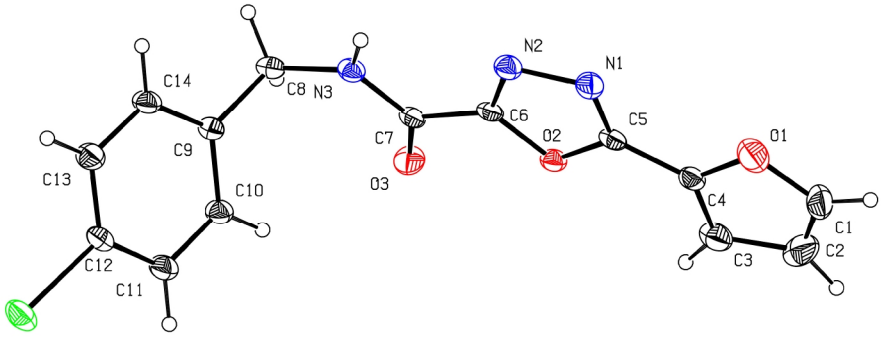

Fig. 1. Molecular structure of the compound 5a

The molecular packing diagram of compound **5a** is displayed in Fig. 2. As can be seen from the packing diagram, there are two orientations of molecules present in the crystal structure, which are connected by two kinds of hydrogen bonds (N(3)–H(3A)⋯N(2) and C(8)–H(8A)⋯O(3)) (See Table 2) and aligned alternately forming a chain along the *b* axis. The chains stack via Van de Waals interactions along the *a* and *c* axes to form a three-dimensional network.

Table 2. Hydrogen Bond Lengths (Å) and Bond Angles (°) of Compound 5a

D–H⋯A	d(D–H)	d(H⋯A)	d(D⋯A)	ÐDHA
N(3)–H(3A)⋯N(2)[a]	0.86	2.21	3.015(6)	155
C(8)–H(8A)⋯O(3)[b]	0.97	2.54	3.360(5)	142

Symmetry codes: (a) –*x*+1, –*y*+2, –*z*+1; (b) –*x*+1, –*y*+1, –*z*+1

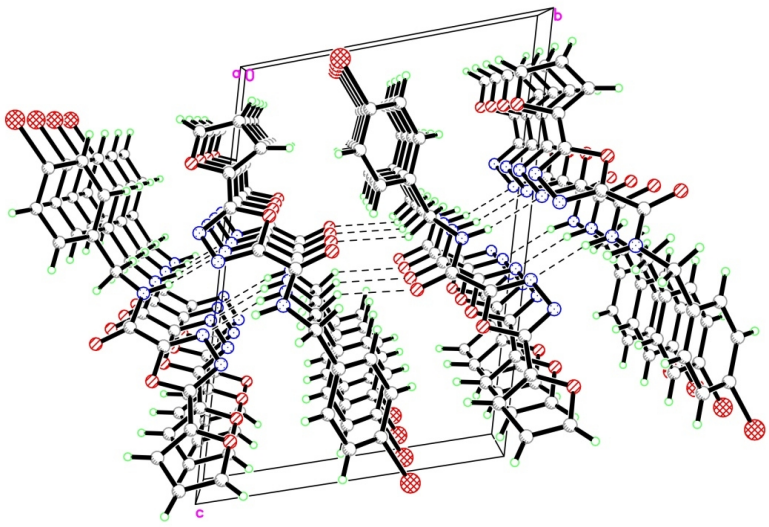

Fig. 2. Perspective view of the molecular packing of compound 5a

Compounds **5a**～**5e** were assayed for their *in vitro* antifungal activities by the mycelia growth inhibition method against seven representative crop pathogenic fungi at 50 mg/L. As shown in Table 3, compounds **5b** and **5c** exhibited prominent antifungal activities against *S. sclerotiorum* with the inhibition rates of 99.3% and 95.1%, respectively, which were equipotent to that of boscalid (100%). Notably, compound **5b** also showed strong inhibitory activity against *A. solani* (90.6%), *R. solani* (80.1%), *B. cinerea* (86.4%) and *F. oxysporum* (70.7%), superior or equipotent to those of boscalid. On the other hand, compounds **5a**, **5d** and **5e** only showed moderate activities to *A. solani*. From these results, it could be deduced that the introduction of electron-withdrawing substituents (-F, **5c** and -Cl, **5b**) could substantially increase the antifungal activities of the derivatives, while the effect of -Br substituent (**5a**) was not obvious compared with -H (**5e**). On the contrary, the introduction of the electron-donating group (-CH_3, **5d**) was not beneficial to the antifungal activity. These results offer a promising scaffold for the discovery of potential antifungal agents against plant pathogenic fungi. The investigations on in-depth structure-activity relationships (SAR) and the antifungal mechanisms of this class of derivatives will be carried out in the future.

Table 3. Antifungal Activities of Compounds 5a～5e

Compd.	R	*R. solani*	*B. cinerea*	*F. oxysporum*	*S. sclerotiorum*	*C. capsici*	*A. solani*	*G. zeae*
5a	-Br	6.4±0.8	11.8±1.3	0	30.6±10.6	22.8±2.7	47.1±5.3	9.7±1.6
5b	-Cl	80.1±1.4	86.4±2.3	70.7±1.6	99.3±0.9	48.3±2.1	90.6±2.5	34.8±3.7
5c	-F	34.8±7.4	52.9±5.2	23.5±3.7	95.1±3.7	13.3±0.9	68.5±1.9	11.7±0.4
5d	-CH_3	11.4±2.4	22.6±0.5	0	0	25.9±1.0	56.5±2.5	17.4±1.2
5e	-H	10.7±1.2	24.3±1.0	5.1±9.5	29.8±8.3	6.1±1.7	45.1±1.9	4.5±1.2
Boscalid		44.2±1.6	75.3±2.0	49.4±3.2	100.0±0.0	15.7±2.1	91.8±1.3	91.7±1.4

REFERENCES

(1) Sparks, T. C.; Lorsbach, B. A. Perspectives on the agrochemical industry and agrochemical discovery. *Pest Manag. Sci.* **2017**, 73, 672–677.

(2) Wang, P. Y.; Wang, M. W.; Zeng, D.; Xiang, M.; Rao, J. R.; Liu, Q. Q.; Liu, L. W.; Wu, Z. B.; Li, Z.; Song, B. A.; Yang, S. Rational optimization and action mechanism of novel imidazole (or imidazolium)-labeled 1,3,4-oxadiazole thioethers as promising antibacterial agents against plant bacterial diseases. *J. Agric. Food Chem.* **2019**, 67, 3535−3545.

(3) Dasgin, S.; Gok, Y.; Celepci, D. B.; Taslimi, P.; Izmirli, M.; Aktas, A.; Gulcin, I. Synthesis, characterization, crystal structure and bioactivity properties of the benzimidazole-functionalized PEPPSI type of Pd(II) NHC complexes. *J. Mol. Struct.* **2021**, 1228, 9.

(4) Mi, Y.; Zhang, J.; Han, X.; Tan, W.; Miao, Q.; Cui, J.; Li, Q.; Guo, Z. Modification of carboxymethyl inulin with heterocyclic compounds: synthesis, characterization, antioxidant and antifungal activities. *Int. J. Biol. Macromol.* **2021**, 181, 572–581.

(5) Tsai, S. E.; Li, S. M.; Tseng, C. C.; Chung, C. Y.; Zeng, Y. H.; Lin, C. C.; Fuh, M. T.; Yang, L. C.; Yang, Y. C.; Wong, F. F. Chlorotrimethylsilane promoted one-flask heterocyclic synthesis of 1,2,4-triazoles from nitrilimines: modeling studies and bioactivity evaluation of LH-21 and Rimonabant analogues. *Bioorg. Chem.* **2020**, 104, 104299.

(6) El Mansouri, A. E.; Oubella, A.; Mehdi, A.; AitItto, M. Y.; Zahouily, M.; Morjani, H.; Lazrek, H. B. Design, synthesis, biological evaluation and molecular docking of new 1,3,4-oxadiazole homonucleosides and their double-headed analogs as antitumor agents. *Bioorg. Chem.* **2021**, 108, 104558.

(7) Briki, K.; Othman, A. A.; Abbassi, M. S.; Lahrech, M. B. Synthesis, characterization and biological activity of Hg(II), Fe(III) complexes with 1,3,4-oxadiazole, 1,2,4-triazole derivatives from L-methionine. *J. Saudi Chem. Soc.* **2020**, 24, 1051–1059.

(8) Li, Y. T.; Yao, W. Q.; Lin, J.; Gao, G. L.; Huang, C.; Wu, Y. Design, synthesis, and biological evaluation of phenyloxadiazole derivatives as potential antifungal agents against phytopathogenic fungi. *Mon. Chem.* **2021**, 152, 121–135.

(9) Yang, S.; Tian, X. Y.; Ma, T. Y.; Dai, L.; Ren, C. L.; Mei, J. C.; Liu, X. H.; Tan, C. X. Synthesis and biological activity of benzamides substituted with pyridine-linked 1,2,4-oxadiazole. *Molecules* **2020**, 25, 3500.

(10) Olmez, N. A.; Waseer, F. New potential biologically active compounds: synthesis and characterization of urea and thiourea derivativpes bearing 1,2,4-oxadiazole ring. *Curr. Org. Synth.* **2020**, 17, 525–534.

(11) Szulczyk, D.; Bielenica, A.; Roszkowski, P.; Dobrowolski, M. A.; Olejarz, W.; Kmiecik, S.; Podsiad, M.; Struga, M. Synthetic transition from thiourea-based compounds to tetrazole derivatives: structure and biological evaluation of synthesized new *N*-(furan-2-ylmethyl)-1H-tetrazol-5-amine derivatives. *Molecules* **2021**, 26, 323.

(12) Wei, M. X.; Yu, J. Y.; Liu, X. X.; Li, X. Q.; Zhang, M. W.; Yang, P. W.; Yang, J. H. Synthesis of artemisinin-piperazine-furan ether hybrids and evaluation of invitro cytotoxic activity. *Eur. J. Med. Chem.* **2021**, 215, 113295.

(13) Khalaf, H. S.; Tolan, H. E. M.; El Bayaa, M. N.; Radwan, M. A. A.; El Manawaty, M.; El Sayed, W. A. Synthesis and anticancer activity of new pyridine-thiophene and pyridine-furan hybrid compounds, their sugar hydrazone, and glycosyl derivatives. *Russ. J. Gen. Chem.* **2020**, 90, 1706–1715.

(14) Kumar, N.; Gusain, A.; Kumar, J.; Singh, R.; Hota, P. K. Anti-oxidation properties of 2-substituted furan derivatives: a mechanistic study. *J. Lumin.* **2021**, 230, 117725.

(15) Kanishchev, O. S.; Lavoignat, A.; Picot, S.; Medebielle, M.; Bouillon, J. P. New route to the 5-((arylthio- and heteroarylthio)methylene)-3-(2,2,2-trifluoroethyl)-furan-2(5H)-ones-key intermediates in the synthesis of 4-aminoquinoline gamma-lactams as potent antimalarial compounds. *Bioorg. Med. Chem. Lett.* **2013**, 23, 6167–6171.

(16) Tighadouini, S.; Radi, S.; Benabbes, R.; Youssoufi, M. H.; Shityakov, S.; El Massaoudi, M.; Garcia, Y. Synthesis, biochemical characterization, and theoretical studies of novel beta-keto-enol pyridine and furan derivatives as potent antifungal agents. *Acs Omega.* **2020**, 5, 17743–17752.

(17) Zhang, X.; Xu, J.; Muhayimana, S.; Xiong, H.; Liu, X.; Huang, Q. Antifungal effects of 3-(2-pyridyl)methyl-2-(4-chlorphenyl) iminothiazolidine against *Sclerotinia sclerotiorum*. *Pest Manag. Sci.* **2020**, 76, 2978–2985.

(18) Tao, P.; Wu, C.; Hao, J.; Gao, Y.; He, X.; Li, J.; Shang, S.; Song, Z.; Song, J. Antifungal application of rosin derivatives from renewable pine resin in crop protection. *J. Agric. Food Chem.* **2020**, 68, 4144–4154.

(19) Zhao, L. X.; Jiang, M. J.; Hu, J. J.; Zou, Y. L.; Cheng, Y.; Ren, T.; Gao, S.; Fu, Y.; Ye, F. Design, synthesis, and herbicidal activity of novel diphenyl ether derivatives containing fast degrading tetrahydrophthalimide. *J. Agric. Food Chem.* **2020**, 68, 3729–3741.

(20) Zhu, S. J.; Xu, S. C.; Jing, W.; Zhao, Z. D.; Jiang, J. X. Synthesis and herbicidal activities of *p*-menth-3-en-1-amine and its Schiff base derivatives. *J. Agric. Food Chem.* **2016**, 64, 9702–9707.

(21) Zhu, J. K.; Gao, J. M.; Yang, C. J.; Shang, X. F.; Zhao, Z. M.; Lawoe, R. K.; Zhou, R.; Sun, Y.; Yin, X. D.; Liu, Y. Q. Design, synthesis, and antifungal evaluation of neocryptolepine derivatives against phytopathogenic fungi. *J. Agric. Food Chem.* **2020**, 68, 2306–2315.

(22) Yu, B.; Zhou, S.; Cao, L.; Hao, Z.; Yang, D.; Guo, X.; Zhang, N.; Bakulev, V. A.; Fan, Z. Design, synthesis, and evaluation of the antifungal activity of novel pyrazole-thiazole carboxamides as succinate dehydrogenase inhibitors. *J. Agric. Food Chem.* **2020**, 68, 7093–7102.

(23) Pedreira, J. G. B.; Philipp, N.; Mark, K.; Tatu, P.; Benedict, T. B.; Michael, F.; Stefan, K.; Stefan, L.; Eliezer, B. Bioisosteric replacement of arylamide-linked spine residues with *N*-acylhydrazones and selenophenes as a design strategy to novel dibenzosuberone derivatives as type I 1/2 p38α MAP kinase inhibitors *J. Med. Chem.* **2020**, 63, 7347–7354.

(24) Yang, Z. H.; Guo, L.; Zhou, C.; Wang, X.; Yu, M.; Min, X.; Yang, K. Synthesis and biological evaluation of nicotinamide derivatives with a diarylamine-modified scaffold as succinate dehydrogenase inhibitors. *J. Pestic. Sci.* **2020**, 45, 1–6.

(25) Zhang, L.; Li, W.; Xiao, T.; Song, Z.; Csuk, R.; Li, S. K. Design and discovery of novel chiral antifungal amides with 2-(2-oxazolinyl)aniline as a promising pharmacophore. *J. Agric. Food Chem.* **2018**, 66, 8957–8965.